Constitutive STAT3 activation in epidermal keratinocytes enhances cell clonogenicity and favors spontaneous immortalization by opposing differentiation and senescence checkpoints

Valeria Orecchia,Gabriella Regis,Beatrice Tassone,Chiara Valenti,Lidia Avalle,Stefania Saoncella,Vincenzo Calautti,Valeria Poli
Constitutive STAT3 activation in epidermal keratinocytes enhances cell clonogenicity and favors spontaneous immortalization by opposing differentiation and senescence checkpoints
EXPERIMENTAL DERMATOLOGY (2014) 24
DOI: 10.1111/exd.12585

Experimental Dermatology ADF

Constitutive STAT3 activation in epidermal keratinocytes enhances cell clonogenicity and favors spontaneous immortalization by opposing differentiation and senescence checkpoints

Journal:	*Experimental Dermatology*
Manuscript ID:	Draft
Manuscript Type:	Regular Article
Date Submitted by the Author:	n/a
Complete List of Authors:	Orecchia, Valeria; Molecular Biotechnology Center, University of Turin, Dept. of Molecular Biotechnology and Health Sciences Regis, Gabriella; Molecular Biotechnology Center, University of Turin, Dept. of Molecular Biotechnology and Health Sciences Tassone, Beatrice; Molecular Biotechnology Center, University of Turin, Dept. of Molecular Biotechnology and Health Sciences Valenti, Chiara; Molecular Biotechnology Center, University of Turin, Dept. of Molecular Biotechnology and Health Sciences Avalle, Lidia; Molecular Biotechnology Center, University of Turin, Dept. of Molecular Biotechnology and Health Sciences Saoncella, Stefania; Molecular Biotechnology Center, University of Turin, Dept. of Molecular Biotechnology and Health Sciences Calautti, Enzo; Molecular Biotechnology Center, University of Turin, Dept. of Molecular Biotechnology and Health Sciences; Poli, Valeria; Molecular Biotechnology Center, University of Turin, Dept. of Molecular Biotechnology and Health Sciences
Keywords:	STAT3, keratinocytes, immortalization, senescence, differentiation

Constitutive STAT3 activation in epidermal keratinocytes enhances cell clonogenicity and favors spontaneous immortalization by opposing differentiation and senescence checkpoints

Valeria Orecchia*, Gabriella Regis*, Beatrice Tassone, Chiara Valenti, Lidia Avalle, Stefania Saoncella, Enzo Calautti, Valeria Poli****

Department of Molecular Biotechnology and Health Sciences, Molecular Biotechnology Center, University of Torino, Italy.

* These authors equally contributed to this work

** Equal contribution and co-corresponding authors:

vincenzo.calautti@unito.it; valeria.poli@unito.it

Department of Molecular Biotechnology and Health Sciences

Molecular Biotechnology Center

University of Torino

Via Nizza 52, 10126 Torino

Italy

Phone: +39-011-6706417

FAX: +39-011-6706432

Abstract

STAT3, a pleiotropic transcription factor acting downstream of cytokines and growth factors, is known to enhance proliferation, migration, invasion and aerobic glycolysis in tumors upon aberrant activation. In the murine epidermis, STAT3 is necessary for experimentally induced carcinogenesis, which is enhanced by the overexpression of the constitutively active STAT3C mutant that also induces robust, psoriasis-like epidermal hyperplasia. We show that STAT3C expression at physiological levels in knock-in mice leads to mild epidermal hyperplasia and attenuated expression of terminal differentiation markers. This delayed differentiation is confirmed in isolated primary epidermal keratinocytes *in vitro*, correlating with enhanced proliferative and clonogenic potential, attenuated senescence and, strikingly, spontaneous immortalization at high frequency. These results suggest that moderate levels of continuous STAT3 activation, which more closely resemble those triggered by chronic inflammation or persistent growth factor stimulation, may favor epidermal carcinogenesis in part by promoting the escape of epidermal progenitor cells from differentiation and senescence checkpoints.

Introduction

Signal Transducers and Activators of Transcription (STAT) factors become activated via tyrosine-phosphorylation (Y-P) and concentrate into the nucleus to regulate the expression of target genes (1). STAT3 can be activated by a wide variety of cytokines, growth factors and oncogenes (2), and plays pleiotropic roles in cell growth and survival including liver regeneration, B lymphocytes proliferation, terminal differentiation and growth arrest in monocytes, lysosome-mediated apoptosis during mammary gland involution, and maintenance of pluripotency in embryonic stem cells (3, 4). STAT3 is considered as an oncogene, being constitutively Y-P in many tumors that often become addicted to its activity (5-7), and required for cell transformation downstream of v-Src and other oncogenes that trigger its Y-P (8, 9). Additionally, overexpression of the constitutively active mutant STAT3C can transform immortalized fibroblasts and epithelial cells (6, 10, 11). In tumors, STAT3 can enhance cell survival and proliferation, promote immune escape, angiogenesis, invasion and metastasis, and modify energy metabolism (12, 13). Moreover, STAT3 is a key player in mediating inflammation-driven tumorigenesis, downstream of chronically high levels of the pro-inflammatory cytokine IL-6 (14), and its activity has been implicated in the maintenance of both normal and cancer stem cells (SC) (13).

The murine skin provides an excellent model to investigate epithelial SC biology and carcinogenesis (15-17). Conditional gene targeting in the epidermis and hair follicles has shown that STAT3 is required both for the initiation and promotion phases in DMBA-TPA skin tumorigenesis and for UVA-induced papilloma development (18, 19). Conversely, keratinocyte-specific STAT3C overexpression (keratin 5-STAT3C TG mice) enhanced both DMBA-TPA and UVA-induced tumorigenesis and elicited the appearance of psoriatic lesions in aging mice (20-22). Moreover, in the aging mouse skin, gains in endogenous JAK/STAT3 signaling downstream of inflammatory cytokines is responsible for impaired functionality of hair follicle SCs (23).

In an effort to model STAT3 activity in tumors, which is usually characterized by low-level, continuous activity rather than by overexpression, we have recently generated knock-in mice

expressing physiological levels of STAT3C and shown its *in vivo* oncogenic potential (24). $STAT3^{C/C}$ mice die between four and six weeks of age due to the development of immune-mediated myocarditis (25), and could therefore not be used for studies on adult mice. Making use of $STAT3^{C/C}$ mouse embryonal fibroblasts (MEFs), we could show that constitutively active STAT3 enhances proliferation and promotes resistance to apoptosis and senescence, correlating with a switch towards aerobic glycolysis and with tumor transformation upon spontaneous immortalization, thus acting as a first hit in malignant transformation (26, 27).

Here, we analyze the outcome of STAT3C expression in the skin and show that continuous aberrant STAT3 activity, which can be observed under chronic inflammatory conditions, alters the pool of clonogenic and proliferative precursors in the epidermis promoting, like in fibroblasts, pre-oncogenic features.

Materials and methods

Mice and treatments

STAT3$^{C/C}$ mice were generated as described (28) and maintained in the transgenic unit of the MBC with water and food *ad libitum*. Genetic screening was performed by PCR as previously described (28). Procedures were conducted in conformity with national and international laws and policies as approved by the Faculty Ethical Committee.

Cell culture, treatment and viral transduction

Primary mKCs were isolated from 3-day-old mice and cultured in low calcium medium (50 μM $CaCl_2$) as described (29, 30). 12-*O*-tetradecanoylphorbol-13-acetate (TPA) in DMSO was used at 100ng/ml (31, 32). Cells were passaged at subconfluency for serial propagation and immortalization analysis. For morphological analyses of cultured cells Axiovert 200M Zeiss microscope was used. Colony forming efficiency assay (CFE) were performed as described (33) with minor modifications. Briefly, 10^4 cells were plated on a feeder layer of lethally irradiated 3T3-J2 and after 12 days colonies were fixed and stained with Rhodamine-B, and scored under a dissecting microscope. Total colonies were calculated as a percentage of total plated cells (number of colonies x 100/number of cells plated).

pLKO.1 lentiviral vectors (Open Biosystems, Huntsville AL, USA) contained the following sequences:

scr, CCTAAGGTTAAGTCGCCCTCGCTCGAGCGAGGGCGACTTAACCTTAGG)

shST3-H3: CGACTTTGATTTCAACTACAACTCGAGTTGTAGTTGAAATCAAAGTCG

shST3-H4: CACCATTCATTGATGCAGTTTCTCGAGAAACTGCATCAATGAATGGTG;

lentiviral particles produced by co-transfecting 293T cells with packaging plasmids pCMV-dR8.74 and pMD2.G, harvested and concentrated as described (33), were used to transduce immortalized mKCs for 12 hours, followed by puromycin selection for 48 hours.

IF, immunohistochemistry and image analysis

Skin sections obtained from 3-day-old mice were embedded in OCT (Tissue Tek; American Master Tek Scientific) and fixed in methanol-acetone (1:1) at -20 °C. Cryosections were then processed for IF and IHC staining as described (29) with the following primary antibodies: Loricrin, Filaggrin and Keratin 14 (Covance); p-STAT3 (Cell Signaling and Technology); PCNA (Santa Cruz). For IF samples were counterstained with DAPI and mounted in Vectashield aqueous medium (Vector Labs, Burlingame, CA), then analyzed using a Leica TSCII SP5 confocal microscope (multi-track analysis was used for image acquisition) or a Zeiss Axiobserver microscope with Apotome module. H&E and IHC staining samples were analyzed using Olympus BH2 microscope. For the quantitative analysis of H&E, IF and IHC performed on skin sections, the ImageJ software (NIH) was used.

Real-time PCR

Total RNA was extracted from primary mKCs and reverse-transcribed as previously described (34). Taqman PCR reactions were performed using the Universal Probe Library system (Roche Italia, Monza, Italy) as previously described (34), on an AB 7300 Real Time PCR System (Applied Biosystem, Foster city, CA, USA). The 18S rRNA predeveloped TaqMan assay (Applied Biosystems, Foster city, CA, USA) was used as an internal control. Specific primers and UPL probes used are listed in Supplementary informations.

Western blot analysis

Total protein extracts were obtained in 2%SDS, 50 mM Tris/HCl (pH 7.4) lysis buffer supplemented with 1mM PMSF, 1 mM Na3VO4, 10 mM NaF and 40mg/ml protease inhibitor cocktail (Complete, Roche). Proteins were boiled at 95°C for 5min, cleared by centrifugation (12000 g for 10 min at 4◦C) and the concentration was measured using the Bradford assay (Bio-Rad). Samples were fractionated on SDS/PAGE and transferred on to PVDF membrane (Millipore) for immunoblotting with the following antibodies: total STAT3 (K15, Santa Cruz Biotechnology), actin (Santa Cruz Biotechnology) and horseradish peroxidase-conjugated secondary antibodies

(Sigma-Aldrich). Immunoblots were acquired with the molecular imager ChemiDoc XRS, and densitometric analysis was performed with Quantity One software (Bio-Rad).

Statistical analysis

Data obtained from analysis of cellular growth, CFE assay, IF, IHC and RT-PCR were plotted as mean ± SEM. Results were assessed for statistical significance by a standard two-tailed Student's t test as indicated. p values *P ≤ 0.05, ** P ≤ 0.01, *** P ≤ 0.001.

Results

STAT3$^{C/C}$ newborn mice display epidermal hyperplasia and differentiation abnormalities.

Histological analysis of STAT3$^{C/C}$ newborn mice revealed significantly increased epidermal thickness, suggestive of a mild tissue hyperplasia (Fig. 1a). Consistently, STAT3$^{C/C}$ epidermis displayed ectopic expression of keratin14 in suprabasal cell layers, with a concomitant decreased expression of the granular layer markers filaggrin (FLG) and loricrin (LOR) (15) (Fig. 1b). STAT3 Y-P in the epidermis was increased, confirming enhanced activation, and correlated with higher expression of the proliferative marker PCNA (Fig. 1c). A similar unbalance between proliferation and differentiation markers was confirmed by quantitative RT-PCR analysis of freshly isolated mouse keratinocytes (mKCs) of the two genotypes (Fig. 1d). Thus, constitutively active STAT3 appears not only to enhance the proliferative rate of epidermal mKCs, but also to interfere with their differentiation program.

Delayed TPA-induced differentiation of primary STAT3$^{C/C}$ mKCs.

To test this idea, we evaluated the *in vitro* differentiation ability of STAT3$^{C/C}$ mKCs in response to the *in vitro* differentiating agent TPA (31, 32, 36, 37). Freshly isolated KCs from either STAT3$^{C/C}$ or STAT3$^{WT/WT}$ newborn mice were seeded on collagen-coated dishes for 4 hours before TPA addition, followed by 7 or 24 hours incubation (Fig. 2a). TPA treatment triggered differentiation of STAT3$^{WT/WT}$ mKCs already by 7 hours, as indicated by the sharp reduction in the mRNAs levels for the KRT14 and p63 proliferative markers, paralleled by a strong increase in the levels of the mRNAs for the differentiation markers FLG and LOR. In contrast, downregulation of KRT14 and p63 mRNAs was partial at this time point in STAT3$^{C/C}$ mKCs and, even more strikingly, FLG and LOR mRNAs were unaffected. By 24 hours of treatment however, the levels of these markers became indistinguishable between the two genotypes, indicating that TPA-induced differentiation is only delayed in STAT3$^{C/C}$ mKCs. Taken together, these results are in agreement with the *in vivo*

observations, and suggest that STAT3$^{C/C}$ mKCs possess an intrinsic defect in the response to differentiating stimuli.

Increased proliferative potential and delayed senescence in primary STAT3$^{C/C}$ mKCs.

To directly assess their proliferative potential, primary mKCs were isolated from 3-days old STAT3$^{WT/WT}$ and STAT3$^{C/C}$ mice and serially passaged in low calcium medium (30, 31). Under these conditions, mKCs are unable to withstand prolonged subcultivation, owing to the depletion of proliferating cells by senescence and/or differentiation (38). At early passages, both morphology and proliferation rates of STAT3$^{C/C}$ mKCs were indistinguishable from those of their wild-type counterparts (Fig. 2b, passage (p) 1 and data not shown). As expected, proliferation of STAT3$^{WT/WT}$ mKCs progressively dropped in later passages, correlating with the appearance of morphological features of differentiation and/or senescence, reaching complete proliferative arrest around p 9-10 (Fig. 2b, p7 and p9). In contrast, STAT3$^{C/C}$ cells maintained higher proliferation rates, displaying a typical proliferating morphology with small, tightly packed cells until at least p 7 (compare images at p7 of the two genotypes in Fig. 2b). Accordingly, quantification of senescence-associated β-galactosidase (SA β-gal) activity showed a sharp increase in the numbers of β-gal-positive cells starting at passage 4 in STAT3$^{WT/WT}$ mKCs, while this increase was substantially delayed in STAT3$^{C/C}$ mKCs (Fig. 2c).

Primary STAT3$^{C/C}$ mKCs display enhanced clonogenic potential.

We thus decided to assess the clonogenic potential of freshly isolated mKCs by means of a low density colony forming efficiency (CFE) assay. In this setting, the number of total colonies indicates the overall ability of cells to initiate a culture, whereas colony size and morphology reflects the intrinsic proliferative potential of individual colony-initiating cells (39, 40). Cells were isolated from newborn STAT3$^{WT/WT}$ and STAT3$^{C/C}$ mice, seeded on a layer of mitotically-inactivated feeder cells and cultivated for 12 days (Fig. 3a, c). In order to assess colony size and cell

morphology, colonies were classified into three groups: small colonies (<2 mm); intermediate colonies (2-4 mm); and large colonies (> 4 mm). Small colonies are typically formed of large cells with senescent morphology, while intermediate and large colonies include areas of both senescent and proliferative cells (Fig. 3b). Although the total number of colonies did not differ between primary $STAT3^{C/C}$ and $STAT3^{WT/WT}$ mKCs (Fig. 3d, 1st generation), the two genotypes originated colonies of strikingly different size (Fig. 3a). Whereas in $STAT3^{WT/WT}$ mKCs the majority of colonies fell in the smallest category, $STAT3^{C/C}$ cells generated significantly higher numbers of large colonies with "holoclone-like" morphology, and lower numbers of small-intermediate colonies (Fig. 3a, c). Both intermediate and large $STAT3^{C/C}$ colonies presented large areas of small, tightly packed cells, typical of actively-proliferating mKCs (Fig. 3b). In contrast, $STAT3^{WT/WT}$ intermediate/large colonies were mainly composed of flattened cells with senescent/differentiated appearance. Moreover, despite similar numbers of total colonies in 1st generation assays, when cells where tested for their secondary CFE after one week in culture under standard conditions, $STAT3^{C/C}$ mKCs exhibited significantly higher numbers of total colonies (Fig. 3d, 2nd generation), in addition to maintaining in average a larger colony size (data not shown). Thus, $STAT3^{C/C}$ mKCs contain an enlarged pool of clonogenic cells endowed with high proliferative potential, reminiscent of cultured keratinocyte SCs (holoclones).

$STAT3^{C/C}$ primary mKCs become spontaneously immortalized at high frequency.

Spontaneous immortalization of mKCs is a rare event, unless cells are propagated under specific conditions (38, 41). Accordingly, immortalization was never observed in wild type mKCs when serially passaged in low calcium medium (0 out of 8 individual cultures). In contrast, $STAT3^{C/C}$ cells became immortalized in 50% of the cases (4 out of 8 individual cultures). Immortalization was accompanied by progressively higher numbers of small, tightly-packed cells with undifferentiated morphology and by a remarkable increase in cell clonogenicity (Fig. 4a, b). Immortalized cells expressed high KRT14 and p63 mRNA levels, while FLG and LOR mRNAs were almost

undetectable as compared to STAT3$^{C/C}$ primary mKCs (Fig. 4c), indicating a differentiation roadblock. Consistently, in immortalized STAT3$^{C/C}$ lines, no differentiation morphological changes occurred in response to TPA (Fig. 4d). Of note, both wild type and STAT3$^{C/C}$ KCs similarly acquired the immortal phenotype when propagated under specific inducing conditions (41) (data not shown). These results suggest that constitutive STAT3 activation predisposes mKCs to escape replicative senescence, overcoming a block normally forbidding immortalization under standard culture conditions. Immortalized STAT3$^{C/C}$ mKCs did not exhibit features of transformed cells, as judged by failure to form colonies in soft agar (not shown).

To determine whether STAT3 activity was required to maintain the immortalized cell phenotype, shRNA-mediated STAT3 silencing was performed in the STAT3$^{C/C}$ line 1. Supplementary Fig. 1a shows efficient lentiviral-mediated STAT3 downregulation. STAT3-silenced immortalized cells maintained a tightly packed morphology (Suppl. Fig. 1b), and their clonogenic potential was unaffected (Fig. 4e), suggesting that STAT3 activity favors the immortalization process to become then dispensable. However, STAT3 silencing decreased the expression of both KRT14 and p63 mRNAs, while that of LOR was increased (Fig. 4f), suggesting that STAT3 participates to the regulation of these genes even in immortalized cells.

Discussion

In this study, we show that the expression of physiological levels of constitutively active STAT3 in Stat3C-knockin mouse model (24) alters epidermal homeostasis. Indeed, we observed mild epidermal hyperplasia coupled to impaired keratinocyte terminal differentiation in the suprabasal cell layers of the newborn skin *in vivo*. This is in partial agreement with the strong tissue hyperplasia, reminiscent of human psoriatic lesions, observed in a model of ectopic STAT3C overexpression via a Keratin-5 promoter (22). The less dramatic phenotype observed in our knockin mice is likely due to the lower STAT3C expression levels, which potentially allow the observation of more subtle effects. Indeed, moderate levels of continuous STAT3 activation with minor

increases in expression levels more closely resemble those observed during chronic inflammation or persistent growth factor stimulation.

Keratinocyte differentiation was reduced, but not abrogated in our $STAT3^{C/C}$ mice *in vivo*, suggesting that Stat3C expression may rather affect the choices of epidermal progenitor cells between proliferation and differentiation. $STAT3^{C/C}$ knockin mice die within few weeks from birth (25), thus precluding the analysis of long-term effects of Stat3C expression on epidermal homeostasis or hair follicle cycling *in vivo*. However, by using primary epidermal cells isolated from newborn $STAT3^{C/C}$ mice, we observed a remarkable correspondence with the *in vivo* phenotype, suggesting epidermal cell-autonomous defects. For example, isolated $STAT3^{C/C}$ display altered responses to TPA, a potent inducer of granular layer markers expression and of keratinocyte terminal differentiation *in vitro* (31, 32, 36, 37), with a significant delay in the induction of the LOR and FLG mRNAs, encoding for markers of terminal differentiation, and a symmetrically retarded downregulation of mRNAs encoding for proliferative markers such as p63 and KRT14. Therefore, a persistently elevated STAT3 signaling similar to that observed under chronic inflammatory conditions appears to make keratinocytes intrinsically more resistant to differentiating stimuli by enforcing their stay in the proliferative compartment. This could be due in part to STAT3-dependent activation of proliferative genes such as Cyclin D1 and cMyc in epidermal cells (data not shown), which may oppose the exit of keratinocytes from the cell cycle to engage terminal differentiation. Increased proliferation does not appear however to represent an intrinsic cell-autonomous feature of $STAT3^{C/C}$ mKCs, since their proliferation rates in culture are comparable to those of the wild type controls. The effects of STAT3C on cell proliferation may thus depend on specific tissue environmental contexts, which are likely not entirely recapitulated *in vitro*. On the other hand, STAT3 signaling may enforce keratinocytes within the undifferentiated stem/progenitor compartment by acting on cell fate choices independently of quantitative effects on mitotic rates, similar to what reported in embryonic SCs, where STAT3 has a master role in the maintenance of the "naïve" pluripotent state downstream of LIF (42, 43). This hypothesis is supported by the

finding in CFE assays of a selective increase in the number of cells originating large, undifferentiated colonies with holoclone-like morphology in $STAT3^{C/C}$ mKCs. Moreover, $STAT3^{C/C}$ cells show a significant increase in their long-term proliferative potential upon sustained subcultivation, feature typical of keratinocyte cultures enriched for stem/progenitor cells (44, 45). Finally, $STAT3^{C/C}$ mKCs show a delay in the upregulation of SA β–Gal activity, and fail to acquire a senescent morphology even upon prolonged subcultivation. Protection from senescence and resistance to differentiation play key roles in SC maintenance in the majority of cellular contexts (46, 47). Our data suggest that mild gains in STAT3 activity, by opposing differentiation and/or senescence programs, may favor maintenance of self-renewal ability in cultured epidermal keratinocyte progenitors.

Resistance to both differentiation and senescence may also underlie the remarkable ability of $STAT3^{C/C}$ mKCs to become spontaneously immortalized under culture conditions that normally promote the exhaustion of proliferative potential in murine keratinocytes (38). Interestingly, immortalized $STAT3^{C/C}$ mKCs do not display features of malignant transformation, in contrast with what observed in MEFs, where the expression of STAT3C serves as a first oncogenic hit (27). This difference underscores the tissue and context-specificity of tumor transformation and may partly explain why, in contrast with other chronic inflammatory conditions characterized by high levels of IL-6 and STAT3 activity (14), psoriasis does not appear per se to significantly predispose to developing skin cancer (48).

Our data indicating a role of STAT3 in protection from cell senescence are in agreement with what observed in both $STAT3^{C/C}$ MEF cells and STAT3-addicted tumor cells (26), and consistent with previous work indicating that deletion of Stat3 in the epidermis leads to skin alterations that are reminiscent of anticipated aging (49), which could be attributed in part to a reduced ability of aging SCs to repair tissue damage. Consistently, specific deletion of STAT3 in KCs of the hair follicle bulge leads to significant reduction of DMBA-TPA-induced tumors, correlating with a decrease in

CD34 and α6-integrin double-positive cells in the bulge (50). Interestingly however, STAT3C overexpression under the K5 promoter was also shown to decrease the number of $CD34^+$, $\alpha6^+$ cells, in line with recent work indicating that increased JAK/STAT3 signaling generated by chronic inflammatory conditions contributes to the loss of functional hair follicle SCs occurring in the aging murine skin (23). Thus, like in many other systems, balanced STAT3 activity is required for tissue homeostasis, and depending on the specific context, both gain and loss of activity may contribute to skin aging and SC dysfunctions.

Acknowledgments

The financial support of Telethon, Italy (TCP 06001) (E.C), the Piemonte Region (PISTEM and Converging Technologies Grants) (E.C. and V.P.), the Italian Cancer Research Association (AIRC IG13009), the Ateneo/San Paolo Foundation, the Italian Ministry for University and Research (MIUR PRIN) and the Truus and Gerrit van Riemsdijk Foundation, Liechtenstein to V.P. are gratefully acknowledged. L.A. is the recipient of a FIRC post-doctoral fellowship.

References

1. Schindler C, Levy D E, and Decker T. JAK-STAT signaling: from interferons to cytokines. The Journal of biological chemistry, 2007. 282(28): p. 20059-63.
2. Turkson J and Jove R, *STAT proteins: novel molecular targets for cancer drug discovery*, in *Oncogene*2000. p. 6613-26.
3. Pensa S, Watson C J, and Poli V. Stat3 and the inflammation/acute phase response in involution and breast cancer. J Mammary Gland Biol Neoplasia, 2009. 14(2): p. 121-9.
4. Poli V and Alonzi T. STAT3 Function In Vivo. In: Signal Transducers and Activators of Transcription (STATs), ed. Sehgal P B Levy D E Hirano T. Dordrecht: Springer Netherlands, 2003: 493-512.
5. Al Zaid Siddiquee K and Turkson J. STAT3 as a target for inducing apoptosis in solid and hematological tumors. Cell Res, 2008. 18(2): p. 254-67.
6. Bromberg J F, Wrzeszczynska M H, Devgan G *et al.* Stat3 as an oncogene. Cell, 1999. 98(3): p. 295-303.
7. Kortylewski M, Jove R, and Yu H. Targeting STAT3 affects melanoma on multiple fronts. Cancer Metastasis Rev, 2005. 24(2): p. 315-27.
8. Bromberg J F, Horvath C M, Besser D *et al.* Stat3 activation is required for cellular transformation by v-src. Mol Cell Biol, 1998. 18(5): p. 2553-8.
9. Silva C M. Role of STATs as downstream signal transducers in Src family kinase-mediated tumorigenesis. Oncogene, 2004. 23(48): p. 8017-23.
10. Dechow T N, Pedranzini L, Leitch A *et al.* Requirement of matrix metalloproteinase-9 for the transformation of human mammary epithelial cells by Stat3-C. Proceedings of the National Academy of Sciences of the United States of America, 2004. 101(29): p. 10602-7.
11. Azare J, Leslie K, Al-Ahmadie H *et al.* Constitutively activated Stat3 induces tumorigenesis and enhances cell motility of prostate epithelial cells through integrin beta 6. Mol Cell Biol, 2007. 27(12): p. 4444-53.
12. Demaria M, Camporeale A, and Poli V. STAT3 and metabolism: How many ways to use a single molecule? Int J Cancer, 2014.
13. Avalle L, Regis G, and Poli V. Universal and Specific Functions of STAT3 in Solid Tumours. In: Jak-Stat Signaling : From Basics to Disease, ed. Thomas Decker and Mathias Müller. Springer Vienna, 2012: 305-333.
14. Li N, Grivennikov S I, and Karin M. The unholy trinity: inflammation, cytokines, and STAT3 shape the cancer microenvironment. Cancer Cell, 2011. 19(4): p. 429-31.
15. Blanpain C and Fuchs E. Epidermal homeostasis: a balancing act of stem cells in the skin. Nat Rev Mol Cell Biol, 2009. 10(3): p. 207-17.
16. Abel E L, Angel J M, Kiguchi K *et al.* Multi-stage chemical carcinogenesis in mouse skin: fundamentals and applications. Nat Protoc, 2009. 4(9): p. 1350-62.
17. Boehnke K, Falkowska-Hansen B, Stark H J *et al.* Stem cells of the human epidermis and their niche: composition and function in epidermal regeneration and carcinogenesis. Carcinogenesis, 2012. 33(7): p. 1247-58.
18. Chan K S, Sano S, Kiguchi K *et al.* Disruption of Stat3 reveals a critical role in both the initiation and the promotion stages of epithelial carcinogenesis. J Clin Invest, 2004. 114(5): p. 720-8.
19. Sano S, Chan K S, Kira M *et al.* Signal transducer and activator of transcription 3 is a key regulator of keratinocyte survival and proliferation following UV irradiation. Cancer Res, 2005. 65(13): p. 5720-9.

20. Chan K S, Sano S, Kataoka K *et al.* Forced expression of a constitutively active form of Stat3 in mouse epidermis enhances malignant progression of skin tumors induced by two-stage carcinogenesis. Oncogene, 2008. 27(8): p. 1087-94.
21. Kim D J, Angel J M, Sano S *et al.* Constitutive activation and targeted disruption of signal transducer and activator of transcription 3 (Stat3) in mouse epidermis reveal its critical role in UVB-induced skin carcinogenesis. Oncogene, 2009. 28(7): p. 950-60.
22. Sano S, Chan K S, Carbajal S *et al.* Stat3 links activated keratinocytes and immunocytes required for development of psoriasis in a novel transgenic mouse model. Nat Med, 2005. 11(1): p. 43-9.
23. Doles J, Storer M, Cozzuto L *et al.* Age-associated inflammation inhibits epidermal stem cell function. Genes & development, 2012. 26(19): p. 2144-53.
24. Barbieri I, Pensa S, Pannellini T *et al.* Constitutively active Stat3 enhances neu-mediated migration and metastasis in mammary tumors via upregulation of Cten. Cancer Res, 2010. 70(6): p. 2558-67.
25. Camporeale A, Marino F, Papageorgiou A *et al.* STAT3 activity is necessary and sufficient for the development of immune-mediated myocarditis in mice and promotes progression to dilated cardiomyopathy. EMBO Mol Med, 2013. 5(4): p. 572-90.
26. Demaria M, Giorgi C, Lebiedzinska M *et al.* A STAT3-mediated metabolic switch is involved in tumour transformation and STAT3 addiction. Aging (Albany NY), 2010. 2(11): p. 823-42.
27. Demaria M, Misale S, Giorgi C *et al.* STAT3 can serve as a hit in the process of malignant transformation of primary cells. Cell Death Differ, 2012. 19(8): p. 1390-7.
28. Maritano D, Sugrue M L, Tininini S *et al.* The STAT3 isoforms alpha and beta have unique and specific functions. Nat Immunol, 2004. 5(4): p. 401-9.
29. Calautti E, Li J, Saoncella S *et al.* Phosphoinositide 3-kinase signaling to Akt promotes keratinocyte differentiation versus death. The Journal of biological chemistry, 2005. 280(38): p. 32856-65.
30. Hennings H, Michael D, Cheng C *et al.* Calcium regulation of growth and differentiation of mouse epidermal cells in culture. Cell, 1980. 19(1): p. 245-54.
31. Calautti E, Missero C, Stein P L *et al.* fyn tyrosine kinase is involved in keratinocyte differentiation control. Genes & development, 1995. 9(18): p. 2279-91.
32. Brissette J L, Li J, Kamimura J *et al.* The product of the mouse nude locus, Whn, regulates the balance between epithelial cell growth and differentiation. Genes & development, 1996. 10(17): p. 2212-21.
33. Saoncella S, Tassone B, Deklic E *et al.* Nuclear Akt2 opposes limbal keratinocyte stem cell self-renewal by repressing a FOXO-mTORC1 signaling pathway. Stem Cells, 2013.
34. Schiavone D, Dewilde S, Vallania F *et al.* The RhoU/Wrch1 Rho GTPase gene is a common transcriptional target of both the gp130/STAT3 and Wnt-1 pathways. Biochem J, 2009. 421(2): p. 283-92.
35. Macias E, Rao D, and Digiovanni J. Role of stat3 in skin carcinogenesis: insights gained from relevant mouse models. J Skin Cancer, 2013. 2013: p. 684050.
36. Dlugosz A A and Yuspa S H. Coordinate changes in gene expression which mark the spinous to granular cell transition in epidermis are regulated by protein kinase C. The Journal of cell biology, 1993. 120(1): p. 217-25.
37. Yuspa S H, Ben T, Hennings H *et al.* Divergent responses in epidermal basal cells exposed to the tumor promoter 12-O-tetradecanoylphorbol-13-acetate. Cancer Res, 1982. 42(6): p. 2344-9.
38. Hager B, Bickenbach J R, and Fleckman P. Long-term culture of murine epidermal keratinocytes. J Invest Dermatol, 1999. 112(6): p. 971-6.
39. Jensen K B, Driskell R R, and Watt F M. Assaying proliferation and differentiation capacity of stem cells using disaggregated adult mouse epidermis. Nat Protoc. 5(5): p. 898-911.

40. Barrandon Y and Green H. Three clonal types of keratinocyte with different capacities for multiplication. Proceedings of the National Academy of Sciences of the United States of America, 1987. 84(8): p. 2302-6.
41. Romero M R, Carroll J M, and Watt F M. Analysis of cultured keratinocytes from a transgenic mouse model of psoriasis: effects of suprabasal integrin expression on keratinocyte adhesion, proliferation and terminal differentiation. Exp Dermatol, 1999. 8(1): p. 53-67.
42. Niwa H, Ogawa K, Shimosato D *et al.* A parallel circuit of LIF signalling pathways maintains pluripotency of mouse ES cells. Nature, 2009. 460(7251): p. 118-22.
43. Stuart H T, van Oosten A L, Radzisheuskaya A *et al.* NANOG amplifies STAT3 activation and they synergistically induce the naive pluripotent program. Curr Biol, 2014. 24(3): p. 340-6.
44. Barrandon Y, Grasset N, Zaffalon A *et al.* Capturing epidermal stemness for regenerative medicine. Semin Cell Dev Biol, 2012. 23(8): p. 937-44.
45. De Luca M, Pellegrini G, and Green H. Regeneration of squamous epithelia from stem cells of cultured grafts. Regen Med, 2006. 1(1): p. 45-57.
46. Behrens A, van Deursen J M, Rudolph K L *et al.* Impact of genomic damage and ageing on stem cell function. Nat Cell Biol, 2014. 16(3): p. 201-7.
47. Jones D L and Rando T A. Emerging models and paradigms for stem cell ageing. Nat Cell Biol, 2011. 13(5): p. 506-12.
48. Pouplard C, Brenaut E, Horreau C *et al.* Risk of cancer in psoriasis: a systematic review and meta-analysis of epidemiological studies. J Eur Acad Dermatol Venereol, 2013. 27 Suppl 3: p. 36-46.
49. Sano S, Itami S, Takeda K *et al.* Keratinocyte-specific ablation of Stat3 exhibits impaired skin remodeling, but does not affect skin morphogenesis. EMBO J, 1999. 18(17): p. 4657-68.
50. Kim D J, Kataoka K, Rao D *et al.* Targeted disruption of stat3 reveals a major role for follicular stem cells in skin tumor initiation. Cancer Res, 2009. 69(19): p. 7587-94.
51. Nardella C, Clohessy J G, Alimonti A *et al.* Pro-senescence therapy for cancer treatment. Nat Rev Cancer, 2011. 11(7): p. 503-11.

Figure legends

Figure 1. STAT3$^{C/C}$ mice display epidermal hyperplasia and reduced differentiation. (a-c) Representative images of skin sections obtained from 3 day-old STAT3$^{C/C}$ and STAT3$^{WT/WT}$ mice. Epi: epidermis; Der: dermis. Grey bars, STAT3$^{WT/WT}$ mice; black bars, STAT3$^{C/C}$ mice. **(a)** H&E staining of paraffin sections (magnification 10X). Bars represent mean ± SEM of the epidermal thickness (n=10 fields/genotype). **(b)** Confocal analysis of cryo-sections subjected to immunofluorescence with the indicated antibodies (red), counterstained with DAPI (blue). Dotted lines indicate the border between epidermis and dermis. Bar: 50µm. Bars represent mean ± SEM thickness of the epidermal layer stained by the corresponding antibody determined as in (a). **(c)** IHC analysis with anti-p-STAT3 and anti-PCNA antibodies (magnification 20X). Bars represent the mean positive area per epidermal area ± SEM (n= 5 fields/genotype), measured using the Metamorph Image Software (Zeiss). **(d)** Taqman RT-PCR on total RNA from primary STAT3$^{C/C}$ and STAT3$^{WT/WT}$ mKCs, represented as mean ± SEM of the values normalized to the 18SrRNA internal control. n=3 per genotype. KRT14, keratin 14; FLG, filaggrin; LOR, loricrine; INV, involucrin.

Figure 2. Cultured primary STAT3$^{C/C}$ mKCs display enhanced lifespan and delayed senescence. (a) Freshly isolated mKCs from STAT3$^{C/C}$ (black bars) and STAT3$^{WT/WT}$ (grey bars) mice were seeded for 4 hours, then treated with DMSO (-) or TPA for 7 or 24 hours. Total RNA was analyzed by Taqman RT-PCR for the indicated markers of epidermal proliferation (KRT14, p63) and differentiation (LOR, FLG). Data are mean ± SEM of 3 samples/genotype. **(b-c)** mKCs of the indicated genotypes were serially cultured for the indicated passages (p) and analyzed **(b)** by phase contrast imaging. All STAT3$^{WT/WT}$ cells were dead by p9 (+). Magnification 10X. **(c)** Percentage of SA β-gal^{+} STAT3$^{WT/WT}$ and STAT3$^{C/C}$ cells at the indicated passages, calculated on at least 300 cells per genotype (n=3) from 2 independent experiments.

Figure 3. STAT3$^{C/C}$ mKCs display increased colony forming efficiency. (a-d) CFE assay. 4*10^3 primary STAT3$^{C/C}$ and STAT3$^{WT/WT}$ mKCs were seeded under clonogenic conditions. After 12 days colonies were fixed and stained with Rodamine-B **(a)**. **(b)** Phase contrast images of representative colonies (Magnification 10X). **(c)** Bars represent the mean percentage of colonies of the indicated sizes ± SEM of at least 100 colonies/genotype, from two independent experiments performed in duplicate (n=4 per genotype). **(d)** The total colony numbers of CFE assay were determined on 1st and 2nd generation (grey bars, STAT3$^{WT/WT}$; black bars, STAT3$^{C/C}$), and reported to the unitary value of 1st generation STAT3$^{WT/WT}$ cells.

Figure 4. Spontaneous immortalization of STAT3$^{C/C}$ mKCs. (a,b) Representative images of STAT3$^{C/C}$ KCs at passage 1 (P, left) and after spontaneous immortalization (I, right). **(a)** Phase contrast images of cultuterd cells; **(b)** Rhodamine-B stained CFE assay. **(c)** Total RNA from P (black bars) or I (striped bars) STAT3$^{C/C}$ mKCs was analyzed by Taqman RT-PCR for the indicated markers. Data are mean ± SEM of 3 samples per condition. **(d-f)** Immortalized STAT3$^{C/C}$ mKCs were: **(d)** exposed to DMSO (-) or TPA for 24h **(**phase contrast images are shown); transduced with lentiviral vectors expressing scrambled (scr) or STAT3-directed shRNA (Stat3 H3) and **(e)** analyzed for colony forming efficiency (Rhodamine-B staining) or **(f)** for the expression of the indicated markers by Taqman RT-PCR. Data are mean ± SEM of the values from at least 3 independent experiments, normalized to the 18SrRNA internal control and reported to those obtained with the scr samples.

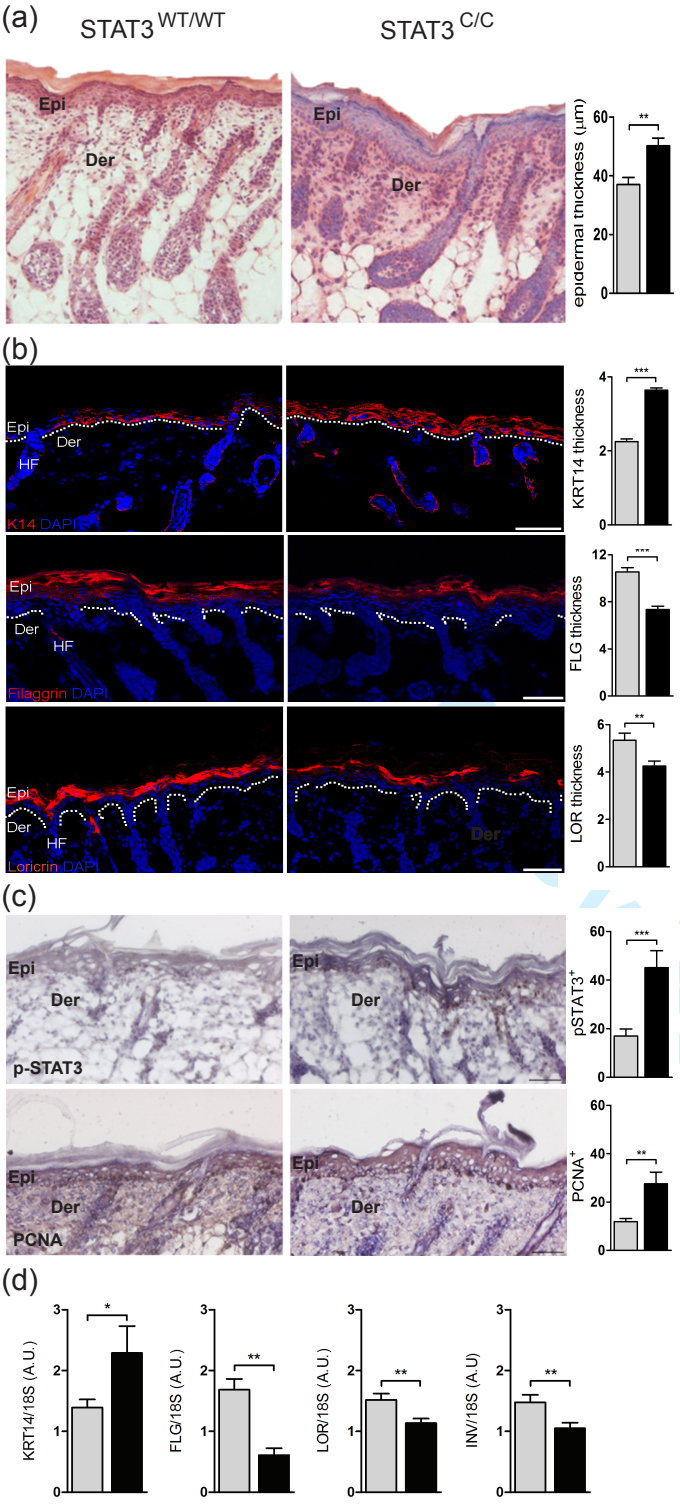

Fig.1

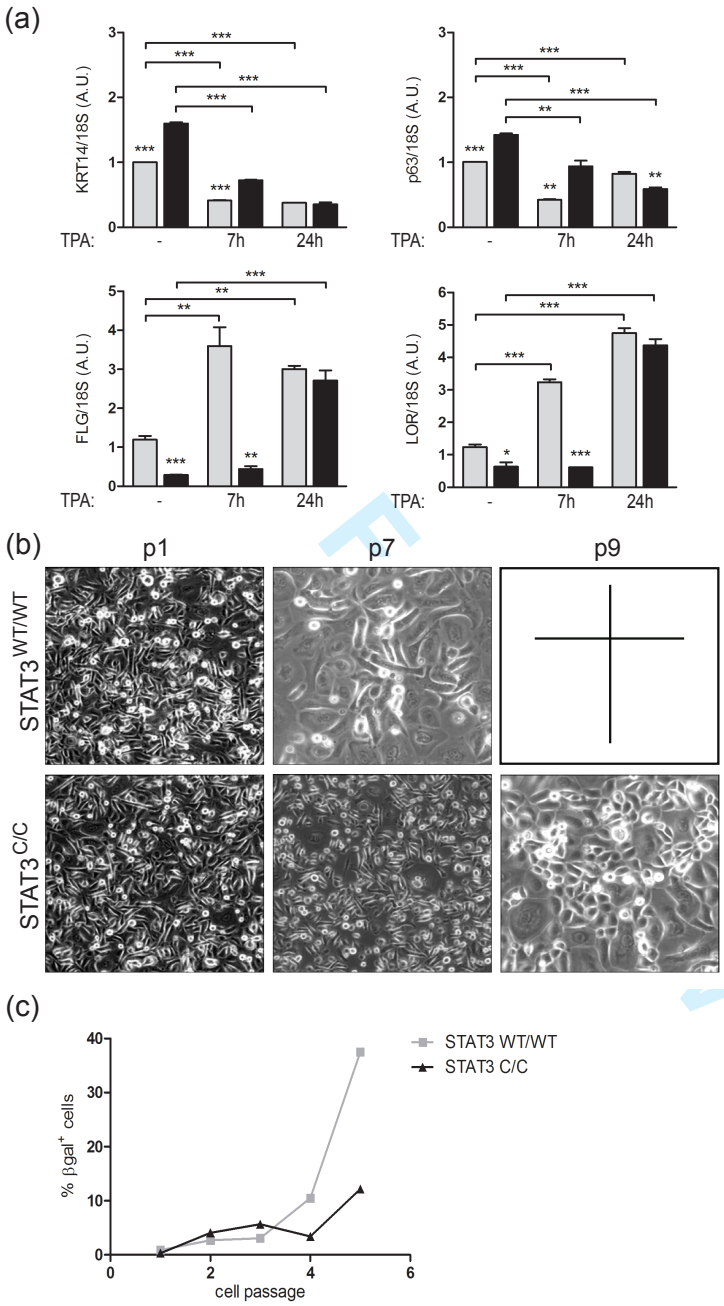

Fig.2

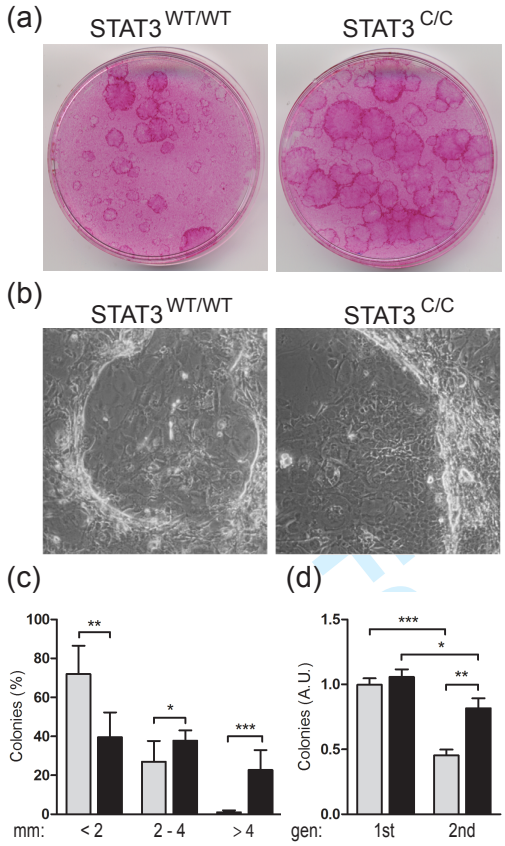

Fig.3

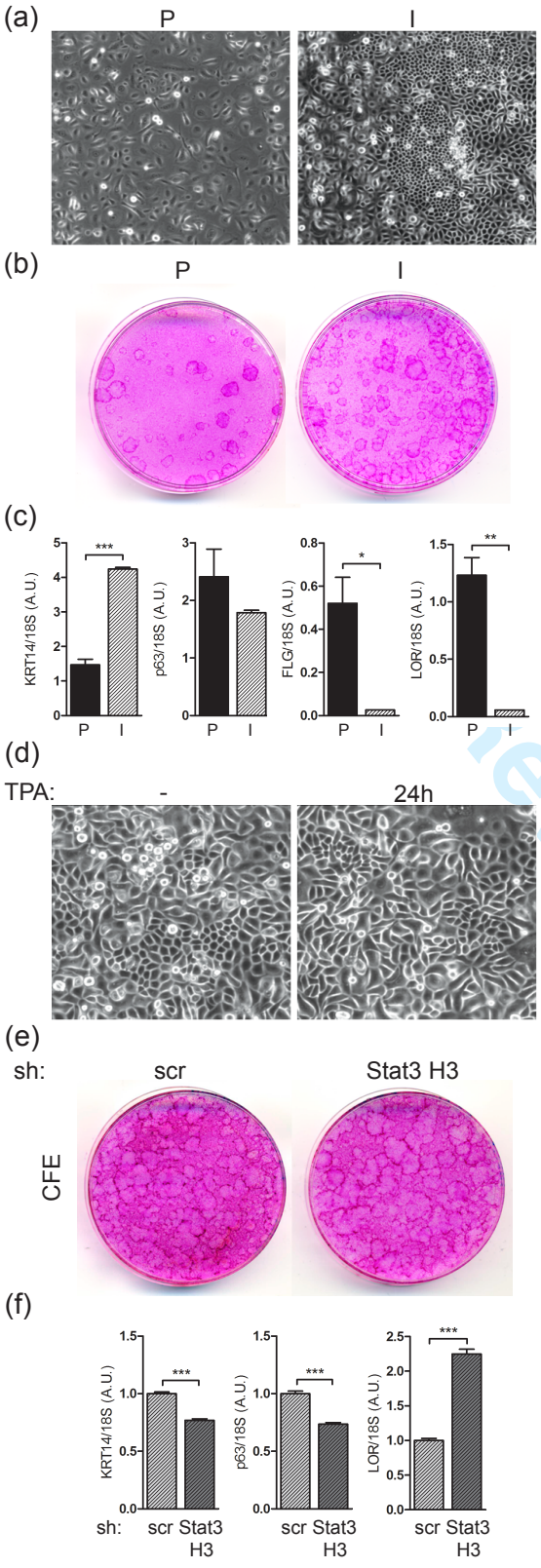

Fig.4

Supplementary informations

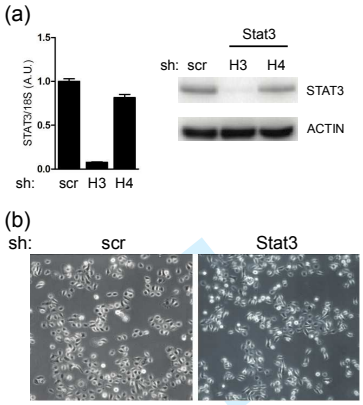

Supplementary Fig.1

Figure S1. STAT3 silencing in immortalized STAT3$^{C/C}$ mKCs. Immortalized STAT3$^{C/C}$ mKCs at p13 were transduced with lentiviral vectors expressing two independent shRNA constructs targeted to STAT3 (shST3-H3, shST3-H4) and a scrambled control shRNA (scr). **(a)** The histograms represent Taqman RT-PCR analysis of STAT3 mRNA levels in the transduced cells (mean values ± SEM) of 3 independent experiments as normalized to the 18S internal control and reported to those obtained with the scr controls. The right panel shows Western blot analysis with antibodies against STAT3 and actin as a loading control. The shST3-H3 induces a nearly 90% STAT3 downregulation and was used for the experiments shown in Figure 4 (e-f). **(b)** Phase contrast images of transduced cells grown at subconfluency.

Specific primers and UPL probes:

KRT14, Fw–atcgaggacctgaagagcaa, Rv–tcgatctgcaggaggacatt, UPL #83;

FLG, Fw–gcctctgcaggtggactg, Rv–gaatggactggctgtcactg, UPL #20;

LOR, Fw–ggttgcaacggagacaaca, Rv–catgagaaagttaagcccatcg, UPL #11;

INV, Fw–ggatctgcctgatcaaaagtg, Rv–cagctgctgcttttgtgg, UPL#71;

p63, Fw–ggaaaacaatgcccagactc, Rv–aatctgctggtccatgctgt, UPL #45;

SOCS3, Fw–atttcgcttcgggactagc, Rv–aacttgctgtgggtgaccat, UPL #83;

STAT3, Fw–tggcaccttggattgagag, Rv–caacgtggcatgtgactctt, UPL #71;